Using N-Heterocyclic Carbenes as Weak Equatorial Ligands to Design Single-Molecule Magnets: Zero-Field Slow Relaxation in Two Octahedral Dysprosium(III) Complexes

Jérôme Long, Dmitry Lyubov, Galina Gurina, Yulia Nelyubina, Fabrice Salles, Yannick Guari, Joulia Larionova, Alexander Trifonov

Using N-heterocyclic carbenes as weak equatorial ligands to design Single-Molecule Magnets: zero-field slow relaxation in two octahedral dysprosium(III) complexes.

Jérôme Long*,[a,b] Dmitry M. Lyubov,[c,d] Galina A. Gurina,[d] Yulia V. Nelyubina,[c] Fabrice Salles,[a] Yannick Guari,[a] Joulia Larionova[a] and Alexander A. Trifonov*[c,d]

[a] ICGM, Univ. Montpellier, CNRS, ENSCM, Montpellier, France.

[b] Institut Universitaire de France (IUF), 1 rue Descartes, 75231 Paris Cedex 05, France.

[c] Institute of Organoelement Compounds of Russian Academy of Sciences, 28 Vavilova str., 119334, Moscow, Russia.

[d] Institute of Organometallic Chemistry of Russian Academy of Sciences, 49 Tropinina str., GSP-445, 630950, Nizhny Novgorod, Russia.

Supporting Information Placeholder

ABSTRACT: We report the synthesis, structures and magnetic investigations of two new octahedral dysprosium complexes, based on the original N-Heterocyclic Carbene (NHC) tridentate bisphenoxide ligand, of respective formula *mer*-[DyL(THF)$_2$Cl] (1) and *mer*-[DyL(THF)$_3$][BPh$_4$] (2) (L = 1,3-bis(3,5-di-*tert*-butyl-2-oxidophenyl)-5,5-dimethyl-3,4,5,6-tetrahydropyrimidin-1-ium-2-ide). The short Dy−O distances in the axial direction in association with the weak donor ability of the NHC-moiety provides a suitable environment for slow relaxation of the magnetization, overcoming the previous SMMs based on NHC ligands.

Lanthanide complexes have become ubiquitous in the research activity devoted to the investigation of functional molecular materials within the last few decades owing to their important impact for future applications. In particular, Single-Molecule Magnets (SMMs) hold the promise to drive the next generation of high-density storage or quantum computing devices[1-4] since these complexes could retain their magnetization at the molecular scale.[2, 5, 6] To achieve this property, the inherent magnetic anisotropy needs to be exacerbated by controlling the crystal-field (CF) splitting through careful tuning of the coordination environment.

Among these, mononuclear dysprosium systems attract a great deal of attention, owing to a strong axial CF, which could be targeted to stabilize the oblate 4*f* electronic density of the Dy^{3+} ion. Following this approach, essential milestones have been reached within the last few years in two distinct categories of SMMs. Firstly, dysprosium metallocenes involving cyclopentadienyl (Cp^R) derivatives as ligands display reversal barriers of the magnetic moment greater than 1500 cm^{-1} and high blocking temperatures which could even surpass the threshold of liquid nitrogen boiling point.[7-9] The rationale behind such performances implies the linearity of the Cp^R–Dy–Cp^R sequence and short Dy–Cp^R distances that maximize the axiality.

On the other hand, the second group of highly performant SMMs belongs to Werner-type coordination complexes involving alkoxide or aryloxide ligands coordinated in *trans* position to the Dy^{3+} ion and other weak ligands situated in the equatorial plane.[10-15] In particular, pentagonal bipyramid (PB) geometry exhibits reduced Quantum Tunnelling of the Magnetization (QTM) because the D_{5h} local symmetry minimizes the transverse crystal field parameters B_k^q ($q \neq 0$).[6] Yet, large reversal barriers could also be reached in other geometries[15] such as the compressed octahedral one.[16-20] However, although the energy barriers of these coordination complexes are comparable with dysprosium metallocenes, they suffer from weaker blocking temperatures caused by an important Raman relaxation.[21-23] This latter implies metal-ligand vibrational modes and depends on intricate parameters.[2, 5, 24-27] The role of the Cp ligand hapticity in comparison with the simple monodentante alkoxide coordination mode might be important to reduce these molecular vibrations although large separation between the states (*i.e*. large CF splitting) should limit this relaxation.[23, 28] Moreover, the role of the equatorial ligands in dysprosium alkoxide complexes might be particularly relevant to maximize the CF splitting and reduce the QTM.

With that said, we envision that bisphenoxide ligand able to coordinate Dy^{3+} ion with a relatively large (phenoxide)O–Dy–O(phenoxide) angle might be interesting for the SMM design if sufficiently weak ligands could be introduced in

the equatorial plane. Numerous SMMs examples have been reported using for instance Schiff base ligands.[29-31] Yet, the presence of strongly coordinating nitrogens or oxygens in the equatorial plane results in a detrimental effect.

In this sense, it is generally accepted that N-heterocyclic carbene ligands (NHC) are characterized by their strong coordination ability towards metal ions.[32, 33] These neutral moieties are referred as σ-donors and benefit from a great versatility in terms of steric and electronic effects, but their reactivity towards Ln^{3+} ions is far less explored.[34] Thus, there are a relatively low number of examples of lanthanide SMM based on NHC ligands.[35, 36] For instance, the field-induced slow relaxation of the magnetization in homoleptic dysprosium complexes was reported.[37] We notice that the Dy−C distances were found surprisingly long (about 2.5–2.6 Å), suggesting a weak donor ability when employed as polydentate ligands.

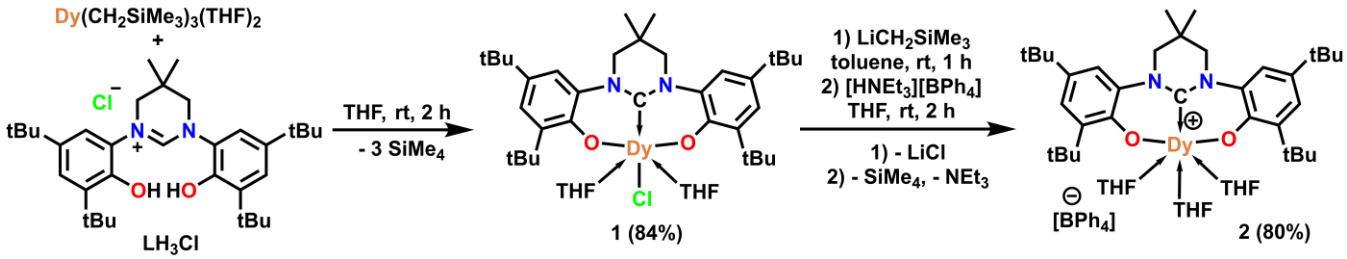

Scheme 1. Synthesis of *mer*-[DyLCl(THF)] (**1**) and *mer*-[DyL(THF)$_3$][BPh$_4$] (**2**).

We report in this communication the synthesis, structures and magnetic investigations of two new heteroleptic octahedral Dy^{3+} complexes involving an original tridentate bisphenolate NHC ligand. This latter incorporating a central NHC-fragment and two peripherical phenoxide moieties provides a relatively linear O−Dy−O angle and a weak Dy-C carbon bond. Both complexes exhibit a zero-field slow relaxation with the performances overcoming previous examples of NHC-based SMMs.

Our synthetic approach relies on the formation of neutral and cationic dysprosium complexes using the designed NHC-bisphenolate [O$^-$,C,O$^-$] ligand (See ESI). The chloride complex *mer*-[DyL(THF)$_2$Cl] (**1**) was obtained *via* the alkane elimination reaction of Dy(CH$_2$SiMe$_3$)$_3$(THF)$_2$ with an equimolar amount of the ligand chlorido salt 1,3-bis(3,5-di-tert-butyl-2-hydroxyphenyl)-5,5-dimethyl-3,4,5,6-tetrahydropyrimidin-1ium chloride (LH$_3$Cl) (Scheme 1). This reaction consists in the cleavage of three Dy−C bonds resulted from the protonolysis by two phenol OH groups and the activation of a relatively acidic C−H bond of the NHC precursor. At the same time, the chloride from the ligand precursor becomes coordinated to the Dy^{3+} ion. Surprisingly, **1** does not react with NaBPh$_4$ (1:1 molar ratio) in THF solution and the starting reagents were completely recovered from the reaction mixture. On the other hand, the Dy−CH$_2$SiMe$_3$ bond in the Dy^{3+} alkyl complex, [DyL(CH$_2$SiMe$_3$)], generated *in situ*, by the salt exchange reaction of **1** and equimolar amount of LiCH$_2$SiMe$_3$, can be easily protonated by the Brønsted acid [HNEt$_3$][BPh$_4$] in THF with the formation of the targeted cationic complex *mer*-[DyL(THF)$_3$][BPh$_4$] (**2**) (Scheme 1).

X-Ray diffraction indicate that **1** and **2** crystallize in the monoclinic *Cc* and triclinic $P\bar{1}$ space groups, respectively, with a unique six-coordinated complex within the asymmetric unit (Table S1). **1** is a neutral complex, in which the coordination sphere of the Dy^{3+} ion incorporates a tridentate L ligand, two THF and one chloride defining a *mer* octahedral arrangement. The shortest distances involve two phenoxide moieties of L, which are disparate and equal to 2.129(7) and 2.152(8) Å for Dy−O1 and Dy−O2, respectively, while the Dy−C bond is considerably longer (2.584(18) Å). The Dy−O(THF) distances are equal to 2.34(1) and 2.369(8) Å and the longest metal-ligand distance corresponds to the Dy−Cl bond with a value of 2.622(5) Å. The O1−Dy−O2 angle deviates significantly from linearity with a value of 150.7(3)°, whereas the (THF)O−Dy−O(THF) one is more linear (171.0(3)°).

In contrast, **2** is a cationic complex incorporating L and three coordinated THF molecules, the charge being compensated by a tetraphenylborate anion. The two Dy−O(phenoxide) distances are almost equivalent with the values of 2.145(6)/2.148(6) Å and a O1−Dy−O2 angle of 149.1(2)°. The Dy−C distance of 2.521(9) Å is slightly shorter with respect to that found in complex **1.**

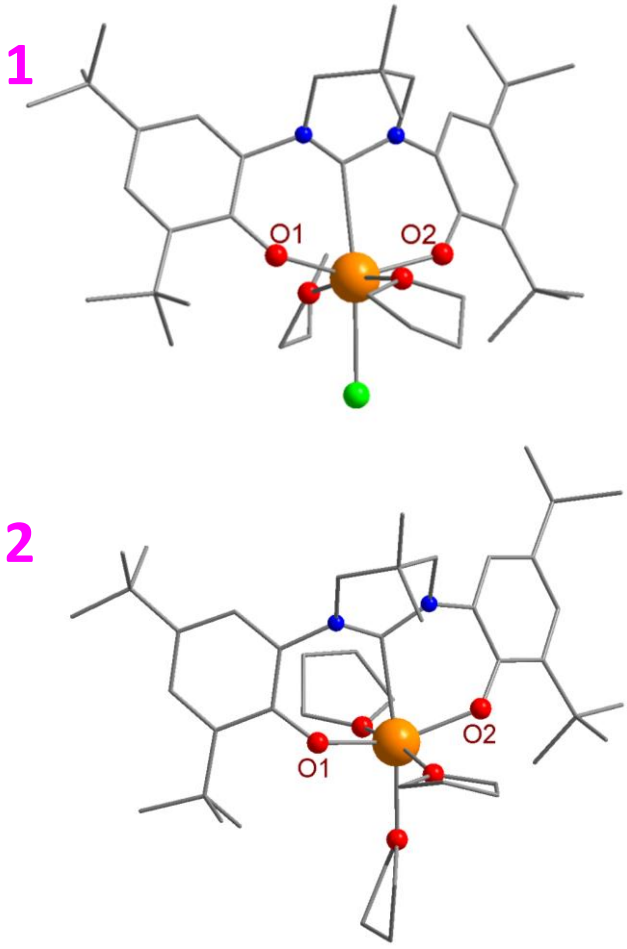

Figure 1. Top: Molecular structure of *mer*-[DyLCl(THF)] (**1**). Bottom: Molecular structure of the cationic part of complex *mer*-[DyL(THF)$_3$][BPh$_4$] (**2**). Colour code: orange, Dy; red, O; grey, C; green Cl. Hydrogen atoms (for **1** and **2**) and the [BPh$_4$]$^-$ moiety (for **2**) have been omitted for clarity.

The Dy−O(THF) distances are ranging between 2.359(6) and 2.387(7) Å. For both complexes, the SHAPE analysis reveals a distorted octahedral geometry (Table S2). Inspection of the crystal packing reveals that the shortest intermolecular Dy⋯Dy distances are equal to 9.846(1) and 11.109(3) Å for **1** and **2**, respectively (Fig. S1).

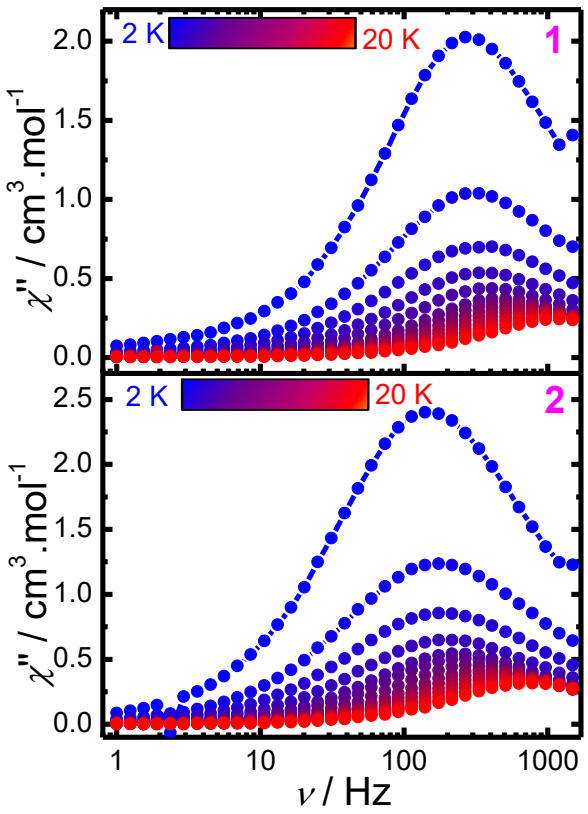

Figure 2. Frequency dependence of the out-of-phase (χ") component of the ac susceptibility for **1** (top) and **2** (bottom) under a zero dc-field.

Static magnetic investigations indicate that the room temperature χT values of 14.27 and 13.08 $cm^3 \cdot K \cdot mol^{-1}$ for **1** and **2**, respectively, are in good agreement with the theoretical value of 14.17 $cm^3 \cdot K \cdot mol^{-1}$ expected for a unique Dy^{3+} ion (Fig. S2). For both complexes, lowering the temperature induces a monotonous χT decrease up to 8 K due to the thermal depopulation of the ± *mJ* levels, then a dramatic drop is observed. At 1.8 K, the field dependence of the magnetization exhibits the typical curve with values of 5.94 and 6.16 *N*β for **1** and **2**, respectively, under a 70 kOe field. Remarkably, the magnetization retention could be evidenced at low temperature by the opening of the hysteresis loops (Fig. S3).

The slow relaxation of the magnetization was further corroborated using alternating current (ac) measurements. Indeed, the frequency dependence of the in-phase (χ') and the out-of-phase (χ'') components of the magnetic susceptibility under a zero dc-field shows a single peak (Fig. 2, Fig S4). The fitted Cole-Cole plots (Fig. S5) give moderate α parameter values (< 0.2) for both complexes, indicating a reasonable distribution of the relaxation times (Table S3 and S4). Extraction of the relaxation time, τ, was performed with CCFIT2[38] to study the relaxation dynamics. At low temperature, τ becomes temperature independent, pointing out a QTM contribution. Besides, the relaxation time at 2 K is about two times greater for **2** with respect to **1** (Fig. 3), suggesting an increased QTM contribution for **1**.

The temperature dependence of τ does not reveal a thermally activated behaviour and consequently, the thermal dependence of was modelled with $\tau^{-1} = CT^n + \tau^{-1}_{QTM}$ (Eq. 1),[37] for which the first and second terms correspond to a Raman and QTM processes, respectively. The best fit parameters (Table 1) reveal rather similar Raman factors for **1** and **2**, whereas QTM substantially differs. To minimize the QTM, the ac susceptibilities under different dc fields were studied (Fig. S6) and the corresponding field dependence of the relaxation time was modelled with $\tau^{-1} = DH^4T + B_1/(1+B_2H^2) + K$ (Eq. 2, Fig. S7, Table S4),[37] for which the first term accounts for the direct process (for Kramers-ion), the second one for the QTM and the *K* constant for the Raman and thermally activated processes. For both complexes, maximization of the relaxation time is obtained using an optimal dc field of 1000 Oe.

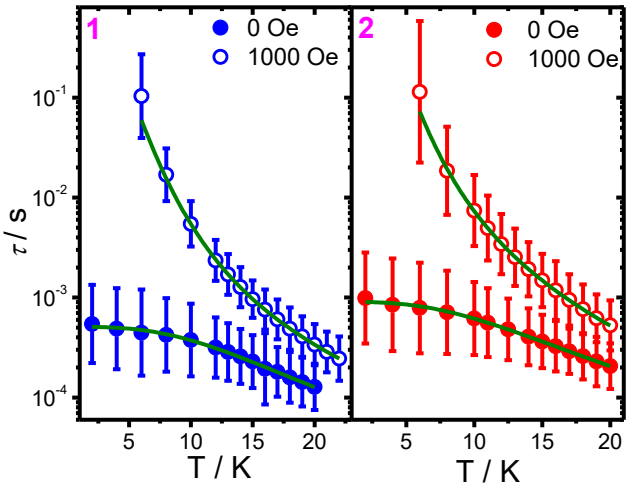

Figure 3. Temperature dependence of the relaxation time for **1** (blue) and **2** (red) using the ac data at 0 Oe and 1000 Oe. The uncertainties were determined from the CC-FIT2 software[38] and green solid lines represent the fit.

The ac data collected under a 1000 Oe dc field (Figs. S8 and S9, Tables S5 and S6) reveals a distinct behaviour with respect to the zero-field data (Fig. 3). It was indeed not possible to fit the data using solely a Raman process and a thermally activated term as $\tau^{-1} = \tau_0^{-1}\exp(-\Delta/kT) + CT^n$ (Eq. 3) was included. To avoid over-parameterization, n was successively fixed to various values until getting the best correlation coefficient.

Table 1: Fit parameters of the temperature dependence of the relaxation time for **1** and **2**.

Compound	Δ (cm^{-1})	τ_0 (s)	n	C ($s^{-1}K^{-n}$)	τ_{QTM} (ms)
1 (0 Oe)	-	-	3.04 ± 0.09	0.6 ± 0.2	0.51 ± 0.02
1 (1000 Oe)	39.9 ± 0.5	(4.4 ± 0.5) × 10^{-5}	3.9*	0.0141 ± 0.0006	-
2 (0 Oe)	-	-	2.85 ± 0.06	0.7 ± 0.1	0.91 ± 0.02
2 (1000 Oe)	32 ± 5	(2.1 ± 0.6) × 10^{-5}	3.9*	0.0090 ± 0.0005	-

**fixed parameter*

Weak but comparable anisotropic barriers of 30–40 cm^{-1} are obtained for both complexes (Table 1). Applying a magnetic field should not modify the anisotropic barrier. Yet, the QTM shortcut caused by the dc field clearly tends to reveal a thermally activated relaxation. Yet, this latter is still governed by a strong Raman process as the absence of a clear linear part suggests (Figure 3). Besides, the large τ_0 values most likely arise from an overlap with the Raman regime.

To gain further insights, *ab initio* calculations at the CASSCF levels were carried out using ORCA (see details ESI).[39] The first excited Kramers doublets are found at about 390 cm^{-1} and 410 cm^{-1} for **1** and **2,** respectively (Table S8). Considering the lack of Orbach relaxation observed in zero dc field, this suggests a strong contribution of the Raman relaxation. The g tensor values shows that the ground doublet exhibits a significant axiality (g_z = 19.91), whereas it decreases for the first excited doublet (g_z = 16.59 for **1** and 16.65 for **2**) with the appearance of non-negligible transverse components. The g_x and g_y values for the ground and first doublets are however found greater for **1** with respect to **2** (Table S8), explaining its increased QTM. This is also confirmed by the values of the transition matrix elements obtained using the SINGLE_ANISO[40] program (Fig. S10). These results suggest that the relaxation is highly limited by the Raman process and proceeds in zero magnetic field through a combination of Raman and QTM. As expected, the anisotropic axes for the ground doublet are found virtually collinear along the O1-Dy-O2 sequence defined by the NHC ligand for both, **1** and **2** (Fig. S11). In line with the distinct charge (**1** is neutral whereas **2** is a cationic), the main difference between the complexes arises from the nature of one co-ligand (chloride *vs*. THF) as well as the distortion induces by different Dy-O^- distances in **1**. Apart from the QTM, the almost similar relaxation features in **1** and **2** could be rationalized as the effect of the negatively charged chloride in **1** is counterbalanced by the relatively short Dy(O-THF) distance in **2**.

In conclusion, two new octahedral dysprosium complexes incorporating a bulky tridentate NHC ligand have been described. They constitute relatively rare examples of lanthanide-based SMMs incorporating a NHC-based ligand. Whereas the presence of two phenoxides ensures the axiality to provide a slow relaxation, the soft donor ability of the carbene may be taken as an advantage to moderate the detrimental influence of the equatorial ligands over the axiality. This clearly contrasts with other ligands, such as for instance Schiff bases, which frequently incorporate strongly coordinating N or O donor atoms. Despite

being limited by a Raman process, the slow relaxation features of **1** and **2** clearly overcome those of other NHC-based SMMs. Thus, appropriate substitution of such unexplored NHC ligands may afford new synthetic routes to design SMMs with enhanced magnetization retention.

ASSOCIATED CONTENT

Supporting Information

Experimental details, crystallographic table, detailed magnetic data and theoretical calculations. This material is available free of charge via the Internet at http://pubs.acs.org.

AUTHOR INFORMATION

Corresponding Author

* E-mail:jerome.long@umontpellier.fr; E-mail: trif@iomc.ras.ru

ACKNOWLEDGMENT

The financial support of the Russian Science Foundation is highly acknowledged (Project № 17-73-30036-П). X-ray diffraction data were collected using the equipment of Center for molecular composition studies of INEOS RAS with the financial support from the Ministry of Science and Higher Education of the Russian Federation. The French authors thank the University of Montpellier and CNRS for funding and PAC of ICGM for measurements. J. Lo also acknowledges the support from the Institut Universitaire de France.

REFERENCES

(1) Luzon, J.; Sessoli, R., Lanthanides in molecular magnetism: so fascinating, so challenging. *Dalton Trans.* **2012,** 41, 13556-13567.
(2) Woodruff, D. N.; Winpenny, R. E. P.; Layfield, R. A., Lanthanide single-molecule magnets. *Chem. Rev.* **2013,** 113, 5110-5148.
(3) Troiani, F.; Affronte, M., Molecular spins for quantum information technologies. *Chem. Soc. Rev.* **2011,** 40, 3119-3129.
(4) Bogani, L.; Wernsdorfer, W., Molecular spintronics using single-molecule magnets. *Nat. Mater.* **2008,** 7, 179-186.
(5) Layfield, R. A.; Murugesu, M., *Lanthanides and Actinides in Molecular Magnetism*. ed.; Wiley: 2015.
(6) Liu, J.-L.; Chen, Y.-C.; Tong, M.-L., Symmetry strategies for high performance lanthanide-based single-molecule magnets. *Chem. Soc. Rev.* **2018,** 47, 2431-2453.
(7) Goodwin, C. A. P.; Ortu, F.; Reta, D.; Chilton, N. F.; Mills, D. P., Molecular magnetic hysteresis at 60 kelvin in dysprosocenium. *Nature* **2017,** 548, 439-442.
(8) Guo, F.-S.; Day, B. M.; Chen, Y.-C.; Tong, M.-L.; Mansikkamäki, A.; Layfield, R. A., Magnetic hysteresis up to 80 kelvin in a dysprosium metallocene single-molecule magnet. *Science* **2018,** 362, 1400-1403.
(9) Randall McClain, K.; Gould, C. A.; Chakarawet, K.; Teat, S. J.; Groshens, T. J.; Long, J. R.; Harvey, B. G., High-temperature magnetic blocking and magneto-structural correlations in a series of dysprosium(iii) metallocenium single-molecule magnets. *Chem. Sci.* **2018,** 9, 8492-8503.
(10) Liu, J.; Chen, Y.-C.; Liu, J.-L.; Vieru, V.; Ungur, L.; Jia, J.-H.; Chibotaru, L. F.; Lan, Y.; Wernsdorfer, W.; Gao, S.; Chen, X.-M.; Tong, M.-L., A Stable Pentagonal Bipyramidal Dy(III) Single-Ion Magnet with a Record Magnetization Reversal Barrier over 1000 K. *J. Am. Chem. Soc.* **2016,** 138, 5441-5450.
(11) Ding, Y.-S.; Chilton, N. F.; Winpenny, R. E. P.; Zheng, Y.-Z., On Approaching the Limit of Molecular Magnetic Anisotropy: A Near-Perfect Pentagonal Bipyramidal Dysprosium(III) Single-Molecule Magnet. *Angew. Chem. Int. Ed.* **2016,** 55, 16071-16074.
(12) Ding, Y.-S.; Yu, K.-X.; Reta, D.; Ortu, F.; Winpenny, R. E. P.; Zheng, Y.-Z.; Chilton, N. F., Field- and temperature-dependent quantum tunnelling of the magnetisation in a large barrier single-molecule magnet. *Nat. Comm.* **2018,** 9, 3134.
(13) Ding, Y. S.; Han, T.; Zhai, Y. Q.; Reta, D.; Chilton, N. F.; Winpenny, R. E. P.; Zheng, Y. Z., A Study of Magnetic Relaxation in Dysprosium(III) Single-Molecule Magnets. *Chem. Eur. J.* **2020,** 26, 5893-5902.
(14) Yu, K.-X.; Kragskow, J. G.; Ding, Y.-S.; Zhai, Y.-Q.; Reta, D.; Chilton, N. F.; Zheng, Y.-Z., Enhancing Magnetic Hysteresis in Single-Molecule Magnets by Ligand Functionalization. *Chem* **2020,** 6, 1777-1793.
(15) Parmar, V.; Mills, D. P.; Winpenny, R., Mononuclear Dysprosium Alkoxide and Aryloxide Single-Molecule Magnets. *Chem. Eur. J.* **2021,** 27, 7625-7645.
(16) Liu, B.-C.; Ge, N.; Zhai, Y.-Q.; Zhang, T.; Ding, Y.-S.; Zheng, Y.-Z., An imido ligand significantly enhances the effective energy barrier of dysprosium(iii) single-molecule magnets. *Chem. Commun.* **2019,** 55, 9355-9358.
(17) Long, J.; Tolpygin, A. O.; Mamontova, E.; Lyssenko, K. A.; Liu, D.; Albaqami, M. D.; Chibotaru, L. F.; Guari, Y.; Larionova, J.; Trifonov, A. A., An unusual mechanism of building up of a high magnetization blocking barrier in an octahedral alkoxide Dy3+-based single-molecule magnet. *Inorg. Chem. Front.* **2021,** 8, 1166-1174.
(18) Ding, X.-L.; Zhai, Y.-Q.; Han, T.; Chen, W.-P.; Ding, Y.-S.; Zheng, Y.-Z., A Local D4h Symmetric Dysprosium(III) Single-Molecule Magnet with an Energy Barrier Exceeding 2000 K**. *Chem. Eur. J.* **2021,** 27, 2623-2627.
(19) Long, J.; Tolpygin, A.; Lyubov, D.; Udilova, N.; Cherkasov, A.; Nelyubina, Y. V.; Guari, Y.; Larionova, J.; Trifonov, A., High Magnetization Reversal Barriers in Luminescent Dysprosium Octahedral and Pentagonal Bipyramidal Single-Molecule Magnets based on fluorinated alkoxides ligands. *Dalton Trans.* **2021,** 50, 8487-8496.
(20) Ding, X.-L.; Luo, Q.-C.; Zhai, Y.-Q.; Zhang, Q.; Tian, L.; Zhang, X.; Ke, C.; Zhang, X.-F.; Lv, Y.; Zheng, Y.-Z., Switching the Local Symmetry from D5h to D4h for Single-Molecule Magnets by Non-Coordinating Solvents. *Inorganics* **2021,** 9.
(21) Giansiracusa, M. J.; Kostopoulos, A. K.; Collison, D.; Winpenny, R. E. P.; Chilton, N. F., Correlating blocking temperatures with relaxation mechanisms in monometallic single-molecule magnets with high energy barriers (Ueff > 600 K). *Chem. Commun.* **2019,** 55, 7025-7028.
(22) Castro-Alvarez, A.; Gil, Y.; Llanos, L.; Aravena, D., High performance single-molecule magnets, Orbach or Raman relaxation suppression? *Inorg. Chem. Front.* **2020,** 7, 2478-2486.
(23) Reta, D.; Kragskow, J. G. C.; Chilton, N. F., Ab Initio Prediction of High-Temperature Magnetic Relaxation Rates in Single-Molecule Magnets. *J. Am. Chem. Soc.* **2021,** 143, 5943-5950.

(24) Tang, J.; Zhang, P., Lanthanide Single-Ion Molecular Magnets. In *Lanthanide Single Molecule Magnets*, Springer Berlin Heidelberg: Berlin, Heidelberg, 2015; pp 41-90.
(25) Ungur, L.; Chibotaru, L. F., Strategies toward High-Temperature Lanthanide-Based Single-Molecule Magnets. *Inorg. Chem.* **2016,** 55, 10043-10056.
(26) Lunghi, A.; Totti, F.; Sessoli, R.; Sanvito, S., The role of anharmonic phonons in under-barrier spin relaxation of single molecule magnets. *Nat. Comm.* **2017,** 8, 14620.
(27) Escalera-Moreno, L.; Baldoví, J. J.; Gaita-Ariño, A.; Coronado, E., Spin states, vibrations and spin relaxation in molecular nanomagnets and spin qubits: a critical perspective. *Chem. Sci.* **2018,** 9, 3265-3275.
(28) Garlatti, E.; Chiesa, A.; Bonfà, P.; Macaluso, E.; Onuorah, I. J.; Parmar, V. S.; Ding, Y.-S.; Zheng, Y.-Z.; Giansiracusa, M. J.; Reta, D.; Pavarini, E.; Guidi, T.; Mills, D. P.; Chilton, N. F.; Winpenny, R. E. P.; Santini, P.; Carretta, S., A Cost-Effective Semi-Ab Initio Approach to Model Relaxation in Rare-Earth Single-Molecule Magnets. *J. Phys. Chem. Lett.* **2021**, 8826-8832.
(29) Gebrezgiabher, M.; Bayeh, Y.; Gebretsadik, T.; Gebreslassie, G.; Elemo, F.; Thomas, M.; Linert, W., Lanthanide-Based Single-Molecule Magnets Derived from Schiff Base Ligands of Salicylaldehyde Derivatives. *Inorganics* **2020,** 8.
(30) Long, J.; Basalov, I. V.; Forosenko, N. V.; Lyssenko, K. A.; Mamontova, E.; Cherkasov, A. V.; Damjanović, M.; Chibotaru, L. F.; Guari, Y.; Larionova, J.; Trifonov, A. A., Dysprosium Single-Molecule Magnets with Bulky Schiff-base Ligands: Modification of the Slow Relaxation of the Magnetization by Substituent Change. *Chem. Eur. J.* **2019,** 25, 474-478.
(31) Chin, W.; Lin, P.-H., Influence of Energy Barriers in Triangular Dysprosium Single-Molecule Magnets through Different Substitutions on a Nitrophenolate-Type Coligand. *Inorg. Chem.* **2018,** 57, 12448-12451.
(32) Hopkinson, M. N.; Richter, C.; Schedler, M.; Glorius, F., An overview of N-heterocyclic carbenes. *Nature* **2014,** 510, 485-496.
(33) Huynh, H. V., Electronic Properties of N-Heterocyclic Carbenes and Their Experimental Determination. *Chem. Rev.* **2018,** 118, 9457-9492.
(34) Arnold, P. L.; Casely, I. J., F-Block N-Heterocyclic Carbene Complexes. *Chem. Rev.* **2009,** 109, 3599-3611.
(35) Arnold, P. L.; Liddle, S. T., F-block N-heterocyclic carbene complexes. *Chem. Commun.* **2006**, 3959-3971.
(36) Arnold, P. L.; Casely, I. J.; Turner, Z. R.; Carmichael, C. D., Functionalised Saturated-Backbone Carbene Ligands: Yttrium and Uranyl Alkoxy–Carbene Complexes and Bicyclic Carbene–Alcohol Adducts. *Chem. Eur. J.* **2008,** 14, 10415-10422.
(37) Meihaus, K. R.; Minasian, S. G.; Lukens, W. W.; Kozimor, S. A.; Shuh, D. K.; Tyliszczak, T.; Long, J. R., Influence of pyrazolate vs N-heterocyclic carbene ligands on the slow magnetic relaxation of homoleptic trischelate lanthanide(III) and uranium(III) complexes. *J. Am. Chem. Soc.* **2014,** 136, 6056-6068.
(38) Reta, D.; Chilton, N. F., Uncertainty estimates for magnetic relaxation times and magnetic relaxation parameters. *Phys. Chem. Chem. Phys.* **2019,** 21, 23567-23575.
(39) Neese, F., The ORCA program system. *WIREs Computational Molecular Science* **2012,** 2, 73-78.
(40) Ungur, L.; Chibotaru, L. F. *SINGLE_ANISO Program*, 2006-2013.